Proceedings of the European Control Conference 2007
Kos, Greece, July 2-5, 2007

Using dynamical uncertainty models for estimation of uncertainty bounds on power plant performance prediction

P.F. Odgaard & J. Stoustrup & B. Mataji

Abstract— **Predicting the performance of large scale plants can be difficult due to model uncertainties etc, meaning that one can be almost certain that the prediction will diverge from the plant performance with time. In this paper output multiplicative uncertainty models are used as dynamical models of the prediction error. These proposed dynamical uncertainty models result in an upper and lower bound on the predicted performance of the plant. The dynamical uncertainty models are used to estimate the uncertainty of the predicted performance of a coal-fired power plant. The proposed scheme, which uses dynamical models, is applied to two different sets of measured plant data. The computed uncertainty bounds cover the measured plant output, while the nominal prediction is outside these uncertainty bounds for some samples in these examples.**

I. INTRODUCTION

Predicting the performance of large scale plants can be difficult due to model uncertainties etc, meaning that one can be almost certain that the prediction will diverge from the actual plant performance with time. A strategy updating the prediction model at each time sample, see [1], will still result in prediction errors and uncertainties, since the model complexity will be limited.

An example on such a plant is a power plant, where prediction of the plant performance can be used to identify possible unfortunately situations due to problematic combinations of operating conditions such as (load request, operator set references, known and unknown disturbances). Where as each of the conditions individually might be in the accepted region, nevertheless, the combination of these conditions decreases the performance of the plant or lead to a failure of the plant. An example of such a problem can be found in the coal mills delivering dried and pulverized coal to the furnace in a coal-fired power plant. The problem occurs when high coal flow is requested at the same time as the moisture content in the raw coal is high, and not enough energy is available in the mill to dry the coal particles. These wet coal particles are too heavy to be lifted into the furnace; as a consequence the coal particles will be accumulated in the mill. In [2] a solution to this problem is proposed by bounding the achievable load.

P.F. Odgaard is at KK-Electronic a/s, Pontopidanstræde 101, DK-9220 Aalborg East, Denmark, `pfo@kk-electronic.dk`, he was at Department of Electronic Systems during the research for this paper.

J. Stoustrup is at Section of Automation and Control, Department of Electronic Systems, Aalborg University, Fredrik Bajers Vej 7C, DK-9220 Aalborg East, Denmark, `jakob@control.aau.dk`

B. Mataji is at Dong Energy A/S, Kraftværksvej 53, DK-7000 Fredericia, Denmark, `bama@elsam-eng.com`

The power plant operators do also play an important role in handling such problems. If the operator has access to a prediction of the system performance given the known conditions and planned load/reference changes, the operator could take actions according to the predictions. However, it is known that the available models are uncertain. Consequently the prediction of the future performance deviates from the future system performance of the plant. In [3] and [4] statistically based methods for predicting bounding functions of the uncertainties are presented. These use statistics of past prediction errors for predicting these bounds on the future predictions. In [5] such a statistically based method is applied to a performance problem in a coal-fired power plant, where high moisture content of the raw coal, results in accumulation of coal in the coal mill, which dries and pulverizes the coal before it is blown into the furnace.

For many dynamical systems the model uncertainties are deterministic meaning it would be better to use a dynamical uncertainty model instead of a statistical one. In this paper it is proposed to compute the uncertainties using dynamical uncertainty models as used in H_∞-theory, see [6]. The prediction uncertainty models are computed using output multiplicative uncertainty models. The nominal model is used to predict an expected system behavior. Combining this nominal model prediction with real system data, an uncertain of the prediction is obtained; this uncertainty is modeled by a dynamical model.

The plant used as an example is described in Section II. Section III describes the proposed dynamical uncertainty modeling scheme. The experiments on the power plant data is described in Section IV. The paper is concluded in Section V.

II. PLANT DESCRIPTION

The proposed scheme for predicting the uncertain closed loop system is illustrated by measurement data from a power plant. The model used for predicting the plant performance is a combination of a furnace model found in [7] and [8]. The model is extended with a coal mill model, and controllers. An overview of the model structure can be seen in Fig. 1. The coal mill pulverizes and dries the coal dust, before it is blown into the furnace by the primary air flow. $\dot{m}_{\mathrm{c}}[n]$ denotes the actual coal flow, $\dot{m}_{\mathrm{c,ref}}[n]$ denotes the reference/requested coal flow, $\dot{m}_{\mathrm{pa}}[n]$ denotes the actual primary air flow, $\dot{m}_{\mathrm{pa,ref}}[n]$ denotes the reference/requested primary air flow. Two disturbances to the coal mill are

ISBN: 978-960-89028-5-5

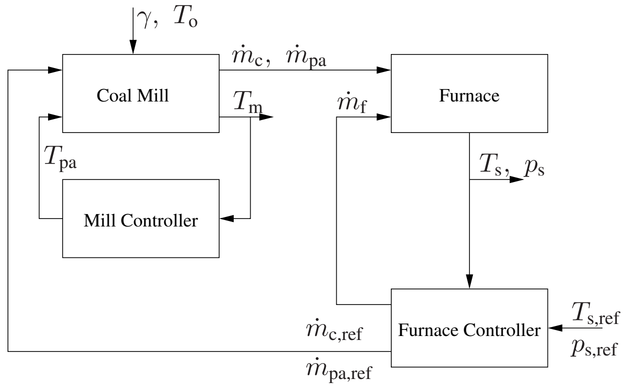

Fig. 1. Illustration of model structure

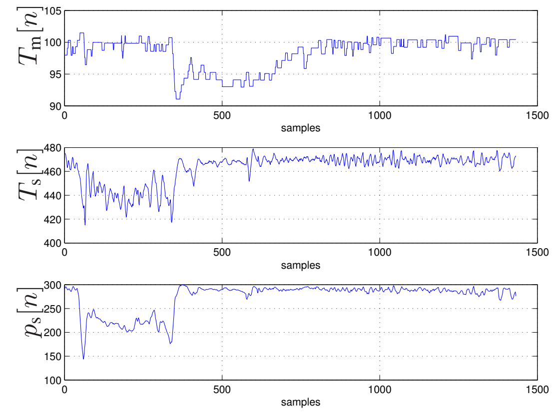

Fig. 2. Plots of the measurements of $T_m[n]$, $T_s[n]$ and $p_s[n]$.

considered, these are the outside temperature, $T_o[n]$ and the coal moisture content, $\gamma[n]$, the temperature of the primary flow. $T_{pa}[n]$, which is used to dry and lift the coal dust in to the furnace, are used to keep the coal dust temperature, $T_m[n]$, at 100°C. In the furnace the coal dust is burned and the hot flue gas is used to heat water to pressurized steam. The steam temperature, $T_s[n]$, and pressure, $p_s[n]$, are used to control the plant, since references are given to those. This control results in coal flow and feed water flow, $\dot{m}_f[n]$, requirements.

The non-linear plant model is subsequently linearized and reduced to a 5 state linear model. The outputs of this linear model are: Coal mill temperature, $T_m[n]$, Steam temperature, $T_s[n]$, and steam pressure, $p_s[n]$. Controlled inputs are reference to steam temperature, $T_{s,ref}[n]$, and reference to steam pressure, $p_{s,ref}[n]$. Another variable in the model which is not controlled or measured is the coal moisture, $\gamma[n]$, which is estimated using the method presented in [9].

In this context acceptable performance of the plant can be defined as selected plant variables being inside some specified bounds, meaning that the performance prediction is used to predict if the plant variable can be expected to be inside these specified bounds in the future. Using only a nominal prediction model does not provide a usable prediction of the future plant performance since uncertainties are not taken into account.

The experimental data from the power plant is sampled with an interval of 60s. The data used in this work contains a load change from 85% load down to 65% load, at sample 65, and up again to 85% load at sample 340. The measured outputs can be seen in Fig. 2. The moisture content, on the other hand, is increasing during the experiment from 14% to 15.5% at the time of the second load change. Consequently not enough energy is available to heat and evaporate the moisture from the pulverized coal, this can be seen by the plot of $T_m[n]$ which decreases below the evaporation point of the moisture, this is an example of non-acceptable performance of the system. A consequence is that these wet coal particles are too heavy to be lifted up to the furnace by the primary air flow. Therefore the coal particles are accumulated inside the coal mill. As a result the plant controllers request a higher coal flow. However, this leads to even more coal being accumulated in the coal mill instead of being blown into the furnace. In this case the moisture content drops again, resulting in more coal being blown into the furnace than requested. Such a situation could result in an overheating of the plant. A safety stop is consequently necessary. Stops of the power plant are highly costly, so these should be avoided if possible. One should also notice that the references are known in advance since these are precomputed for guiding the load.

III. Uncertainty Prediction Method

The two statistically based predictors used in this paper are presented in [3] and [4]. These are based on the same general structure of the predictor, which is illustrated by Fig. 3. Where the system inputs and outputs are used to estimate the present state values, these are fed to the predictor together with system inputs and outputs in order to predict the expected values as well as the uncertainty bounds.

$\hat{\mathbf{x}}[n]$ and $\hat{\mathbf{d}}[n]$ denote the estimated state and disturbance vectors for the time instance n. $\hat{\mathbf{y}}[n]$ is the vector of the predicted system output for the time n, $\epsilon_u[n]$ and $\epsilon_l[n]$ denote respectively upper and lower bounds on system prediction for the time n.

The observer and predictor (prediction model) will subsequently be described in more details.

The close loop model is uncertain with respect to the real system. Consequently an observer is introduced in order to estimate the value of the states at the sample time n.

$$\hat{\mathbf{x}}[n] = \mathbf{\Gamma}\left(\mathbf{u}[n], \mathbf{y}[n], \hat{\mathbf{x}}[n-1]\right), \tag{1}$$

where $\mathbf{\Gamma}$ is an operator representing the observer, and $\hat{\mathbf{x}}[n]$ is the estimated state vector at time n, $\mathbf{u}[n]$ is a vector of plant inputs and $\mathbf{y}[n]$ is a vector of plant outputs.

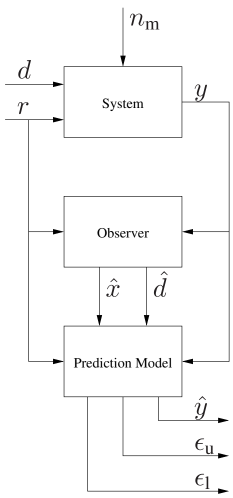

Fig. 3. Overview of the predictor structure, where the observer estimates the present states and in some cases the disturbances as well. The prediction model predicts the system behavior and uncertainties k steps into the future.

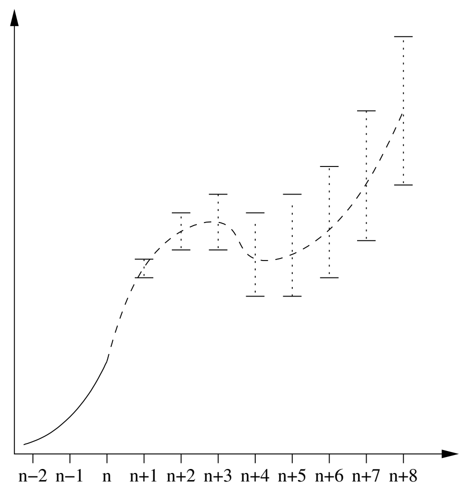

Fig. 4. Illustration of the uncertainty in the prediction. The uncertainty at each prediction step is increased as the number of prediction steps increases.

The estimated states can be used to predict the state and the output vectors a number of samples/steps into the future. In this case the reference is partly known into the future due to prediction of the required plant production, such as power plants where the plant production is planned one day ahead. The disturbance might be known up to time n, i.e. by estimation. Subsequently the reference is denoted $\hat{\mathbf{r}}[n]$ and the disturbance is denoted $\hat{\mathbf{d}}[n]$. The k-step predictor of the output, $\mathbf{y}[n+k|n]$, and states, $\hat{\mathbf{x}}[n+k|n]$, are computed by

$$\hat{\mathbf{x}}[n+1|n] = \mathbf{f}_{\mathrm{m}}\left(\hat{\mathbf{x}}[n], \hat{\mathbf{r}}[n], \hat{\mathbf{d}}[n]\right), \tag{2}$$

where

$$\hat{\mathbf{x}}[n+2|n] = \mathbf{f}_{\mathrm{m}}\left(\hat{\mathbf{x}}[n+1|n], \hat{\mathbf{r}}[n], \hat{\mathbf{d}}[n]\right), \tag{3}$$

continue this recursive process until $\hat{\mathbf{x}}[n+k|n]$ is computed, subsequently compute

$$\hat{\mathbf{y}}[n+k|n] = \mathbf{g}_{\mathrm{m}}\left(\hat{\mathbf{x}}[n+k|n], \hat{\mathbf{r}}[n], \hat{\mathbf{d}}[n]\right). \tag{4}$$

Now when the k-step predictor is defined, it is possible to define a k-step prediction error residual.

$$\mathbf{e}[n+k|n] = \mathbf{y}[n+k] - \hat{\mathbf{y}}[n+k|n]. \tag{5}$$

This prediction residual defined (5) can of course only be computed earliest at sample n.

As previously stated the model is assumed to be uncertain in relation to the real system. It also means that the prediction is expected that the uncertainty increase with increasing prediction horizon. This is illustrated by Fig. 4. The predicted system value is drawn with the dashed line, (from sample $n+1$ to sample $n+8$), the measured system output value is drawn with solid line (sample $n-2$ to n). The uncertainty of the predicted values is marked by the vertical markings, with the small horizontal lines at the ends, the distance between these end markings represent the uncertainty of the specific predicted system value.

The predictor proposed in this paper does predict the future expected output values of the dynamical systems.

In the context mentioned in the introduction (see Section I), it is as well interesting to predict a region in which the output can be expected to be in, e.g. for the operator to see how one can expect the performance of the plant to be given the prespecified conditions and references.

A. Dynamical uncertainty prediction

The approach proposed in this paper uses output multiplicative uncertainty models to model the prediction uncertainties from the nominal prediction model. The output multiplicative model is illustrated in Fig. 5, in which G represents the nominal prediction model fed with $\hat{\mathbf{y}}[n]$, $\hat{\mathbf{r}}[N|n]$ and $\hat{\mathbf{d}}[N|n]$. W is the dynamical weighting function, given by a transfer function, representing the bounding uncertainties and $\Delta[n] \in \{-1:1\}$, which gives all possible uncertainty behaviors. The output of the nominal prediction is $\hat{\mathbf{y}}[N|n]$, and the bounding uncertainty predictions are denoted $\epsilon_{\mathrm{u}}[N|n]$ and $\epsilon_{\mathrm{l}}[N|n]$ for the upper and lower bound respectively. These bounds are defined as the maximal and minimal output of the uncertainty model with the nominal prediction output as input to the uncertainty model.

These uncertainty predictions can be used to compute the upper and lower bounds of the predictions as:

$$\epsilon_{\mathrm{u}}[n+k|n] = \hat{\mathbf{y}}[n+k|n] + \epsilon[n+k|n], \tag{6}$$

$$\epsilon_{\mathrm{l}}[n+k|n] = \hat{\mathbf{y}}[n+k|n] - \epsilon[n+k|n]. \tag{7}$$

W is defined as a filter bounding the frequency content of the past prediction errors. Define a vector of the most

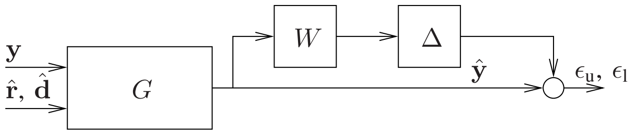

Fig. 5. Illustration of the nominal prediction model and multiplicative output prediction uncertainty model.

recent prediction errors with specified prediction horizon k as

$$\mathbf{E}[q] = \begin{bmatrix} e[q+1|q] & \cdots & e[q+k|k] \end{bmatrix}, \tag{8}$$

for the time n the most recent vector is $\mathbf{E}[n-k]$. The corresponding vectors of the most recent prediction values can be defined as

$$\mathbf{Y}[q] = \begin{bmatrix} y[q+1|q] & \cdots & y[q+k|k] \end{bmatrix}. \tag{9}$$

These pairs of relating $\mathbf{E}[q]$ and $\mathbf{Y}[q]$ vectors are subsequently grouped into different relevant point of operation given by references and disturbances. For each of these point-of-operation groups a filter W is computed as a filter bounding the maximal values for all frequencies of the difference between the prediction vectors and the prediction error vectors.

$$\max_{\omega} \left(\mathrm{FFT}(\mathbf{E}[q]) - \mathrm{FFT}(\mathbf{Y}[q])\right), \ \forall q \in Q_{r,d}, \tag{10}$$

where $Q_{r,d}$ is the set of pairs contained in the specified group of operating points. FFT represent the standard fast Fourier transform, see [10]. The useful type of filter clearly depends on the application, which the scheme is applied on.

In order to simplify the filter parameter identification the order and structure of W can be prespecified. In the example using in Section IV a first order filter is used, and the parameters are found using *Matlab*'s *ident* toolbox.

To be certain that ϵ_{u} and ϵ_{l} bound the prediction uncertainties Δ is set equal to 1. However, in practice this might be conservative. Instead Δ can be adapted to the present prediction uncertainty by

$$\Delta[n] = \frac{\left\|\mathrm{FFT}(\mathbf{R}[n-k]) - \mathrm{FFT}(\mathbf{Y}[n-k])\right\|}{\left\|W\right\|}. \tag{11}$$

The upper bound can subsequently be computed as

$$\hat{\mathbf{y}}[n] + \epsilon[n], \tag{12}$$

and the lower bound

$$\hat{\mathbf{y}}[n] - \epsilon[n], \tag{13}$$

where ϵ in the case where Δ is not corrected, denoted as NC, is computed as

$$\epsilon[n] = \Delta \cdot W\hat{\mathbf{y}}[n], \tag{14}$$

where ϵ in the case where Δ is corrected according to the present prediction uncertainty , denoted as C, is computed as

$$\epsilon[n] = \Delta[n] \cdot W\hat{\mathbf{y}}[n]. \tag{15}$$

This adaptation of $\Delta[n]$ gives a less conservative representation of the uncertainty bounds of the prediction, and whereby gives a much better prediction taking the uncertainties into account.

One should notice that the nominal prediction is not guaranteed to be included in the uncertainty bounds, if the nominal prediction model has a DC-modeling/prediction error.

IV. Experiments

In these experiments the linear model described in Section II is used for the predictor. In addition an optimal unknown input observer is used to estimate the state values, see [11].

These experiments are used to validate that the uncertainty predictor can predict the measured system variables during different plant conditions.

The predictor of the uncertain system is applied to two sets of experimental data from the power plant presented in Section II. Notice that the sample time is 60s. The first set is during the low load, where the system performance is predicted from sample 220 and 80 samples into the future. At this time accumulation of coal is not occurring. The second example contains the problem of coal accumulation, where the system performance is predicted from sample 621 and 80 samples into the future.

The prediction for the first example can be seen in Figs. 6-8, and the plots of the second example are plotted in Figs. 9-11. The order of the plots are $T_{\mathrm{m}}[n]$, $T_{\mathrm{s}}[n]$ and $p_{\mathrm{s}}[n]$. In each of the plots both the non-corrected prediction bounds and the corrected prediction bounds are plotted.

a) Example One: The predictions of $T_{\mathrm{m}}[n]$, $T_{\mathrm{s}}[n]$ and $p_{\mathrm{s}}[n]$ for example one are shown in Figs. 6-8, from these it can be seen that the uncertainty bounds covers all the measured variables, both in the corrected and non-corrected cases. However, the nominal prediction is not covered for all samples. The corrected uncertainty prediction bounds narrow the uncertainty region as expected, and as mentioned previously, still contain the measured values.

b) Example Two: The predictions of $T_{\mathrm{m}}[n]$, $T_{\mathrm{s}}[n]$ and $p_{\mathrm{s}}[n]$ for the second example are shown in Figs. 9-11, from these it can be seen that the uncertainty bounds cover all the measured variables, both in the corrected and non-corrected cases. The corrected uncertainty prediction bounds narrow the uncertainty region as expected, and as mentioned previously, still contain the measured values.

V. Conclusion

In this paper output multiplicative uncertainty models are used as dynamical models of the prediction errors

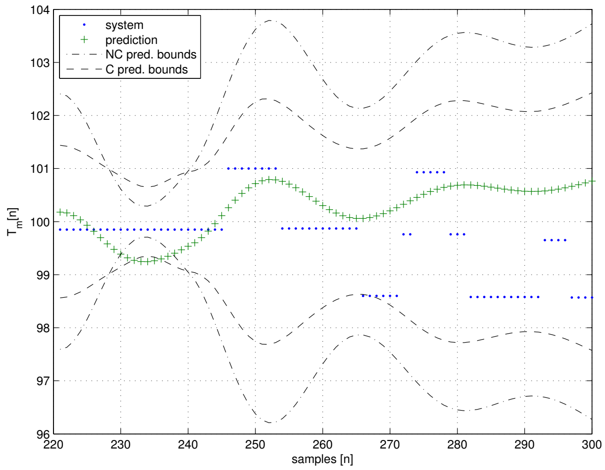

Fig. 6. Plot of $T_{\mathrm{m}}[n]$ for example one. Both the non-corrected (NC) and corrected (C) uncertainty bounds contain the measured values, while the nominal prediction is not contained for all samples.

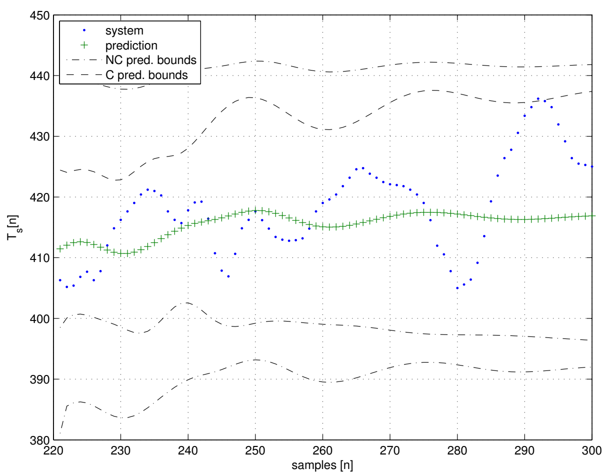

Fig. 7. Plot of $T_{\mathrm{s}}[n]$ for example one. Both the non-corrected (NC) and corrected (C) uncertainty bounds contain the measured values.

for uncertain dynamical predictions. The proposed dynamical scheme for estimating the prediction uncertainty is validated by estimating the prediction uncertainty of the performance of a coal-fired power plant. This prediction method is applied to two different sets of measured data, a set of data for operation under normal conditions and a set of data for a combination of high moisture content and a high load resulting in accumulation of coal in the coal mill. These proposed dynamical uncertainty models result in an upper and lower bound on the predicted performance of the plant. These bounds contain the measured plant output, while the nominal prediction is not covered for all samples for both examples.

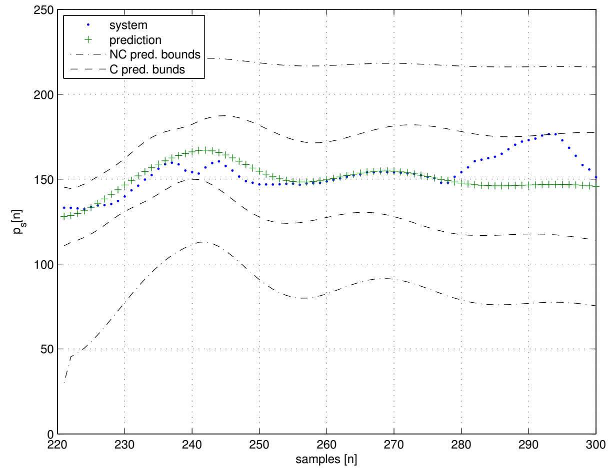

Fig. 8. Plot of $p_{\mathrm{s}}[n]$ for example one. Both the non-corrected (NC) and corrected (C) uncertainty bounds contain the measured values.

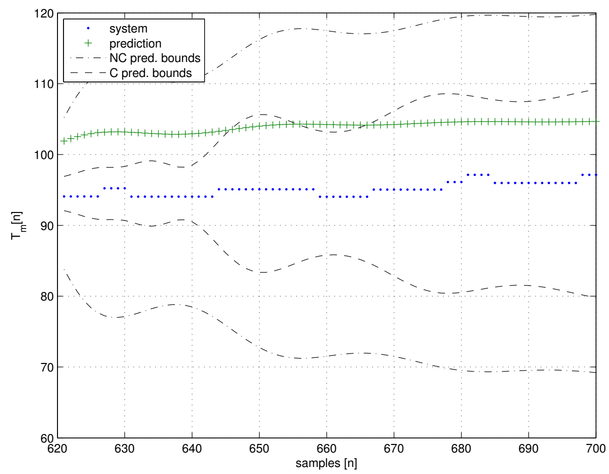

Fig. 9. Plot of $T_{\mathrm{m}}[n]$ for example one. Both the non-corrected (NC) and corrected (C) uncertainty bounds contain the measured values, while the nominal prediction is not contained for all samples.

VI. Acknowledgment

The authors acknowledge the Danish Ministry of Science Technology and Innovation, for support to the research program CMBC (Center for Model Based Control), grant no 2002-603/4001-93.

VII. References

[1] M. Milanese and C. Novara, "Set membership prediction of nonlinear time series," *IEEE Transactions on Automatic Control*, vol. 50, pp. 1655–1669, November 2005.

[2] P. Odgaard, J. Stoustrup, and B. Mataji, "Preventing performance drops of coal mills due to high moisture content," 2007, to appear in proceedings of ECC 2007.

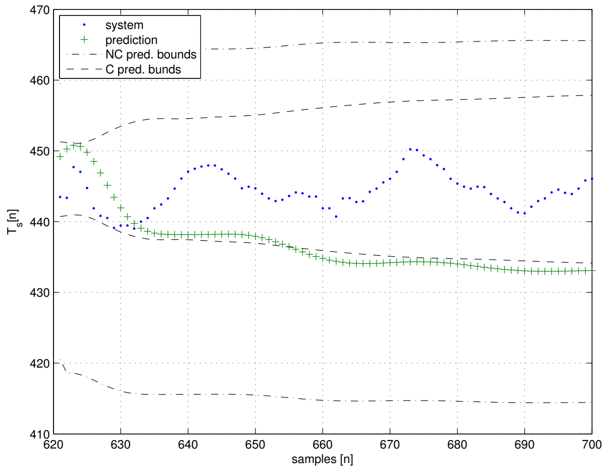

Fig. 10. Plot of $T_\mathrm{s}[n]$ for example two. Both the non-corrected (NC) and corrected (C) uncertainty bounds contain the measured values.

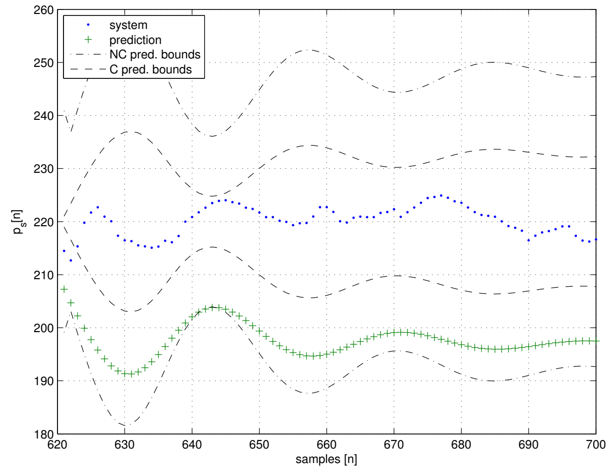

Fig. 11. Plot of $p_\mathrm{s}[n]$ for example one. Both the non-corrected (NC) and corrected (C) uncertainty bounds contain the measured values, while the corrected bounds do not cover the nominal prediction.

[3] ——, "Performance prediction of uncertain plants with disturbances using statistics of uncertainties: applied to a power plant," 2006, submitted for publication.

[4] ——, "Using reference trajectories to predicted uncertain systems: exemplified on a power plant," 2007, to appear in proceedings of ACC 2007.

[5] P. Odgaard, B. Mataji, and J. Stoustrup, "Prediction of lacking control power in power plants using statistical models," 2007, to appear in procedings of ECC 2007.

[6] K. Zhou, J. C. Doyle, and K. Glover, *Robust and optimal control*, 1st ed. Prentice-Hall, Inc., 1996.

[7] J. Bendtsen, J. Stoustrup, and K. Trangbaek, "Multi-dimensional gain scheduling with application to power plant control," in *Proceedings. 42nd IEEE Conference on Decision and Control*, vol. 6, Maui, USA, December 2003, pp. 6553 – 6558.

[8] ——, "Bumpless transfer between advanced controllers with applications to power plant control," in *Proceedings. 42nd IEEE Conference on Decision and Control*, vol. 3, Maui, USA, December 2003, pp. 2059–2064.

[9] P. Odgaard and B. Mataji, "Estimation of moisture content in coal in coal mills," in *Proceedings of IFAC Symposium on Power Plants and Power Systems*, Kananskis, Alberta, Canada, June 2006.

[10] S. Mallat, *A wavelet tour of signal processing*, 2nd ed. Academic Press, 1999.

[11] J. Chen and R. J. Patton, *Robust model-based fault diagnosis for dynamic systems*, 1st ed. Kluwer academic publishers, 1999.